JOURNAL OF AIRCRAFT
Vol. 30, No. 1, Jan.–Feb. 1993

Flowfield in the Vicinity of an F/A-18 Vertical Fin at High Angles of Attack

B. H. K. Lee,* D. Brown,* F. C. Tang,† and M. Plosenski‡
Institute for Aerospace Research, Ottawa, Ontario K1A OR6, Canada

The flowfield behind the vertical fin of a rigid 6% scale F/A-18 model has been investigated in the Institute for Aerospace Research 1.5 m trisonic blowdown wind tunnel. The vortical flow structure was studied with the aid of a 49 pressure-sensor rake mounted on the model support sting. In phase I of this investigation, the rake was located behind the vertical fin at a position which sensed approximately equal amounts of the vortical flow on either side of the fin. In phase II, the rake was positioned between the two vertical fins. Unsteady pressures were sensed by 13 fast-response transducers placed along the horizontal and vertical centerlines of the rake. Spectral, correlation, and probability density analyses were carried out. Results showing angle of attack and Mach number effects are presented.

Nomenclature

C_p = steady pressure coefficient
C_p' = rms value of pressure coefficient, p_{rms}/q
$\bar{c}$ = wing mean aerodynamic chord, 8.29 in.
$\bar{c}_f$ = vertical fin mean aerodynamic chord, 5.03 in.
f = frequency
k = nondimensional frequency, $f\bar{c}/U$
M = Mach number
p_{rms} = rms value of pressure
q = freestream dynamic pressure
$R(X, 0)$ = peak cross-correlation function at X
$R_{e\bar{c}}$ = Reynolds number
U = freestream velocity
X_v, Y_v, Z_v = vortex rake coordinate system
α = angle of attack

I. Introduction

MODERN fighter aircraft which engage in flight at high angles of attack usually suffer severe structural damage in the vertical fins due to the impact of the vortical flow originating from breakdown of the leading-edge extension (LEX) vortices. A number of articles have been published by the authors on wind-tunnel investigations and flight tests of tail buffet on the F/A-18,[1,2] the characteristics and effects of the LEX vortices,[3] and prediction of peak buffet loads.[4]

The provision of aerodynamic-loads data on the vertical fin for the structural engineer to carry out stress analysis and fatigue estimates, may be obtained by direct measurement of steady and unsteady pressures at sufficient points on the fin surfaces. Experiments can be carried out on rigid wind-tunnel models and the measurements used for the full-scale aircraft design after correcting for aeroelastic effects. This is usually a very time-consuming process involving many measurements made at different aerodynamic conditions. Reference 5 describes a method to predict the buffet response in flight tests using rigid-model wind-tunnel data. The induced aerodynamic loads due to structural motion of the aircraft wing were approximated using a linear unsteady aerodynamics theory. The accuracy in determining fin buffet loads depends on the number of transducers installed on the fin for measuring the pressures. For the spatial distributions used in Ref. 1, unpublished results show good agreement with loads measured using strain gauges installed on the fin.

It is highly desirable to be able to obtain approximate estimates of the fin aerodynamic loads without resolving to detailed pressure measurements. Ideally, a prediction method using some features of the flowfield which are dependent on the aircraft configuration and aerodynamic conditions, such as Mach number, Reynolds number, and angle of attack, would be extremely useful. However, before any attempt can be made to formulate a loads model based on the flowfield, it is first necessary to understand the properties of the very complex vortical flow in the vicinity of the vertical fin associated with the bursting of the LEX vortices. A number of studies have been carried out on the vortex-burst phenomenon using water tunnels,[6] laser light sheet measurements,[7] as well as velocity flowfield surveys.[8] The present wind-tunnel investigation is an attempt to obtain quantitative pressure measurements and information on the structure of the vortex flowfield. Measurements were made at subsonic freestream Mach numbers in the Institute for Aerospace Research 1.5 m trisonic blowdown wind tunnel.

II. Model and Instrumentation

The wind-tunnel model used was a sting-mounted 6% scale of the F/A-18; its construction is described in Ref. 1. Figure 1 shows the model location with respect to the wind-tunnel walls at the maximum angle of attack. With a cranked sting, a maximum angle of attack of 33 deg can be obtained. Under

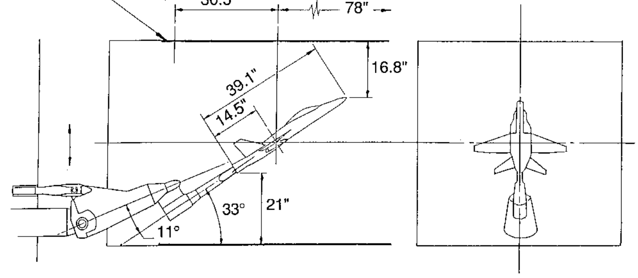

Fig. 1 Schematic of model mounted in wind tunnel.

Received Oct. 12, 1991; revision received Jan. 13, 1992; accepted for publication Jan. 16, 1992.

*Senior Research Officer, High Speed Aerodynamics Laboratory, National Research Council. Member AIAA.

†Associate Research Officer, High Speed Aerodynamics Laboratory, National Research Council.

‡Computer Systems Officer, High Speed Aerodynamics Laboratory, National Research Council.

aerodynamic load, an increment of 2 deg is typically obtained, giving a total angle of attack of 35 deg.

The instrument used to investigate the flowfield in the vicinity of the vertical fin is the vortex rake shown in Fig. 2. In the first phase of this study, the rake was mounted behind the vertical fin at a position to sense an approximately equal amount of vortical flow on either side of the vertical fin. One of the sides of the rake was about 1.2 in. from the aircraft plane of symmetry. The rake was designed to cause low flow blockage and yet be sufficiently rigid to withstand the high-vibration levels from shed vortices of the model aircraft at high angles of attack. The blockage is difficult to estimate a priori; its effect is discussed qualitatively in Sec. III. A. The vortex rake consists of a square array of 49 stagnation pressure measuring tubes supported at 1 in. intervals by two 6 × 6-in. frames. Approximately 3 in. behind the support frames the 0.095-in.-diam tubes (0.071-in. bore) are gathered into a square bundle and housed in a square tube. This was clamped to the model support sting so as to place the face of the array a short distance (approximately 0.6 in.) behind the starboard fin, and oriented at 20 deg to the aircraft model reference line as indicated in Fig. 2.

Thirteen of the 49 active tubes were devoted to dynamic pressure measurements and the remainder to sense steady pressures. The dynamic pressure tubes are distributed on the vertical and horizontal centerlines of the array as indicated in Fig. 2. High-frequency response was obtained by $\frac{1}{16}$-in.-diam Kulite differential pressure transducers cemented just inside the tips of the 0.071-in. bore tubes. The reference side of these transducers was connected by means of a 0.02-in. bore stainless tubing lying inside the 0.071-in. bore tubing of the rake to a pressure manifold located in the base of the sting, which was connected to an external pressure source. Wiring from the transducers was led out alongside the reference pressure tube to electrical connectors mounted on the side of the sting.

The steady stagnation pressure tubes were terminated by cementing short pieces of 0.070-in.-o.d. tubes inside the 0.071-in. bore tubing to form a 1-in.-long tip. The tips were connected to electronically scanned pressure modules that were also housed in the base of the sting by 0.032-in.-o.d., 0.02-in.-i.d. stainless-steel tubing cemented inside the tips of the tubes.

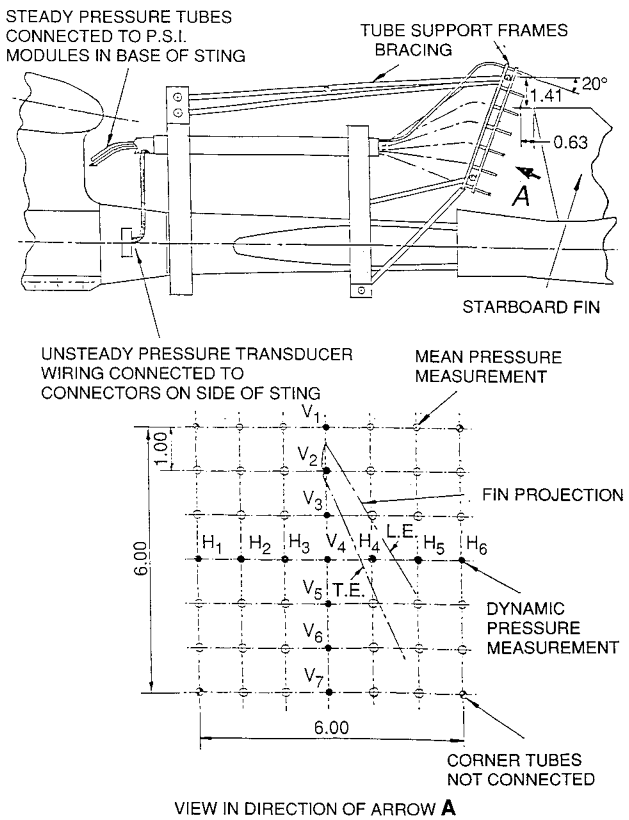

Fig. 2 Vortex rake.

Internal chamfers of 40-deg included-angle were machined in the ends of both dynamic and steady pressure tubes to reduce the directional sensitivity of the rake, since it was required to operate over a 35-deg angle-of-attack range. The tubes became aligned with the freestream direction when the model incidence was 20 deg.

Boundary-layer transition trips were installed on both surfaces of the LEX, wings, fins, and stabilators, and also on the intakes and forebody of the model.

In the second phase of the study, the probe was positioned between the vertical fins in such a way that its vertical centerline corresponded to the model plane of symmetry. The face of the array of total pressure tubes was inclined at 30 deg to the aircraft model reference line, and located at approximately 0.6 in. behind the fins.

III. Results and Discussion

Most of the results given in this article were obtained from data recorded during the first phase of the investigation. In particular, results at $M = 0.6$ are analyzed in detail. Some results at $M = 0.6$ and 0.8 from the second phase are also presented to illustrate the effects of Mach number on the structure of the flowfield. Results at three values of α only, namely, 25, 30, and 35 deg are discussed. They represent the flow phenomena that are of the most interest for the Mach number range investigated. The mean position of the center of the vortical flow is outboard of the vertical fin at $\alpha = 25$ deg and in the vicinity of the fin at $\alpha > 25$ deg for $M = 0.6$. All measurements were carried out with the LEX fences "on." The leading- and trailing-edge flaps were deflected at 35 deg and 0 deg, respectively. The horizontal stabilator angle was set at -9 deg.

The Reynolds numbers based on wing mean aerodynamic chord were approximately 3.5×10^6 and 4.15×10^6 at $M = 0.6$ and 0.8, respectively.

A. Steady Total Pressure Contours

With the rake mounted behind the vertical fin, the vortical flow total pressure contour lines can be mapped. Figure 3 shows the time-averaged constant total pressure expressed in coefficient form for three values of α. The view is looking downstream from the nose of the aircraft, and the vertical line at $Y_v = 6$ in. does not correspond to the plane of symmetry but is about 1.2 in. to the left. At $\alpha = 25$ deg the center of the low-pressure region is located outboard of the vertical fin. At $\alpha = 30$ deg a low-pressure region is also detected inboard of the fin indicating the presence of a second vortex. At $\alpha = 35$ deg this low-pressure region increases in size and the vortex center shifts upwards.

Moving the vortex rake to a symmetrical position between the vertical fins gives total pressure contours as shown in Fig. 4 for the same three values of α. The Reynolds number and dynamic pressure are practically the same as those in Fig. 3. If the starboard fin is lined up in these figures with those obtained with the rake behind the vertical fin, the contours match fairly well except for a few contours at $\alpha = 25$ deg near the inboard surface. This may be due to the fact that as α decreases, the influence of the rake on the vortical flow becomes more significant. No direct study of the influence of the rake on the vortical flow has been performed since such an investigation is very difficult to carry out. However, some indirect study of the rake influence was obtained from the fin unsteady pressures with the rake on and off. Unpublished results show that the pressures were modified by the presence of the rake, but the differences was less significant at higher values of α, e.g., above 30 deg at $M = 0.6$. At these high values of α the vortex-burst positions are quite far upstream. Rake interference is still present but is not as important as in

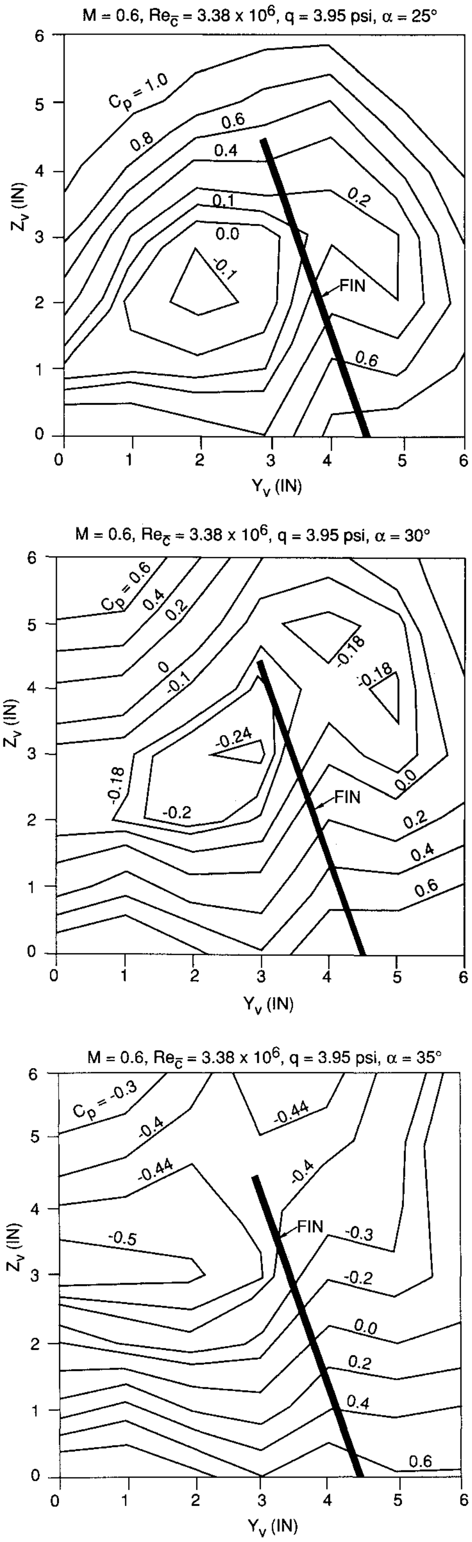

Fig. 3 Total pressure contours behind vertical fin.

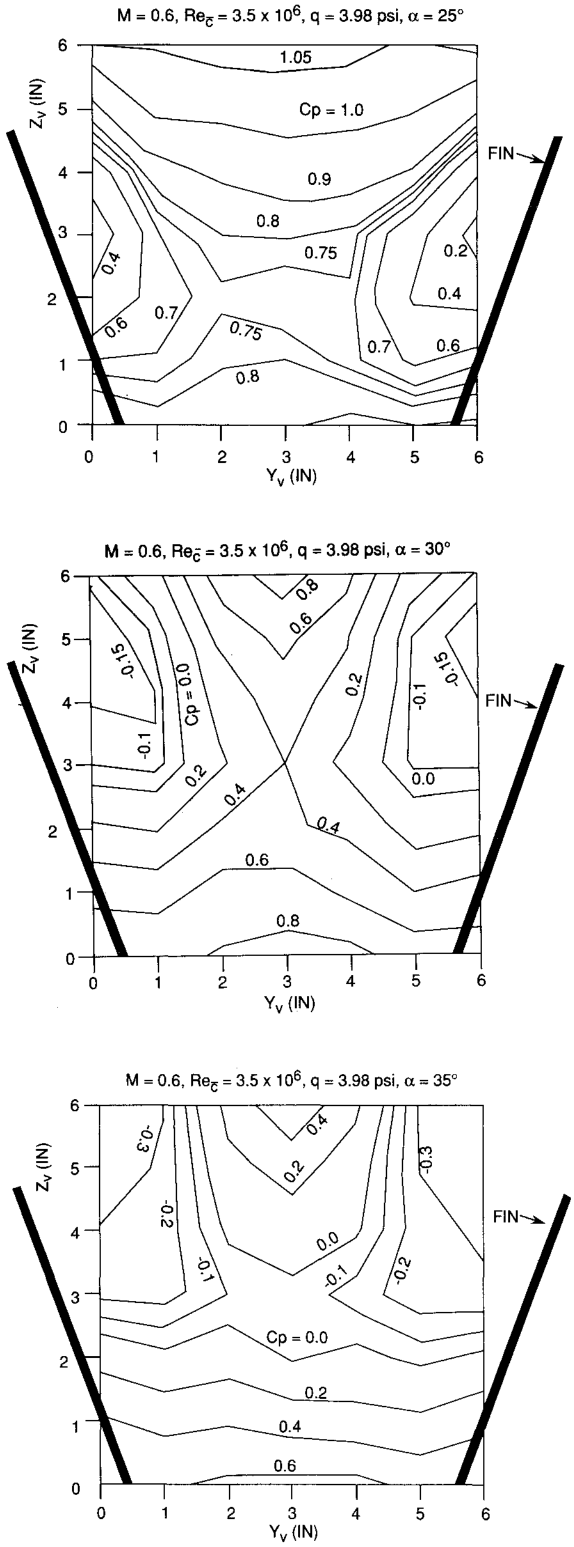

Fig. 4 Total pressure contours between vertical fins.

the lower α cases. Integrated normal force coefficients for the fin with and without the rake are given in Ref. 3 at $M = 0.6$. These data show that the differences are larger at the lower angles of attack. At $\alpha = 10$ deg a maximum difference in normal force coefficient of 0.05 was observed. The present results, though not absolutely representative of the undisturbed flowfield, still give an indication of its structure.

B. Unsteady Pressure Measurements

To study the time-varying properties of the vortical flowfield, some commonly used statistical methods in unsteady aerodynamics were applied. The data from the 13 unsteady pressure signals are presented as power spectral density plots along the vertical column and horizontal row of transducers shown in Figs. 5 and 6 for the three values of α considered.

In Fig. 5, V_1 is the transducer located at the top of the rake and V_7 is at the bottom. At $\alpha = 30$ deg, V_4 is very close to the center of the vortex. A broad peak with centered reduced frequency k of approximately 0.5 is observed at V_1 for $\alpha = 30$ deg and also at V_2 and V_7. They are indistinct at some locations along the vertical column of transducers. It should be noted that the vertical scale is very compressed.

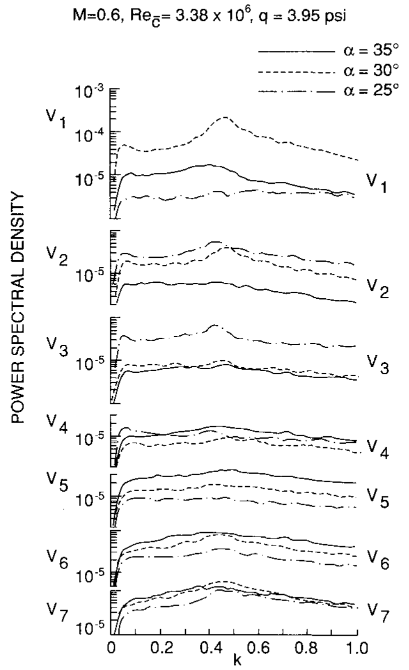

Fig. 5 Power spectral density of vortex rake vertical array of transducers.

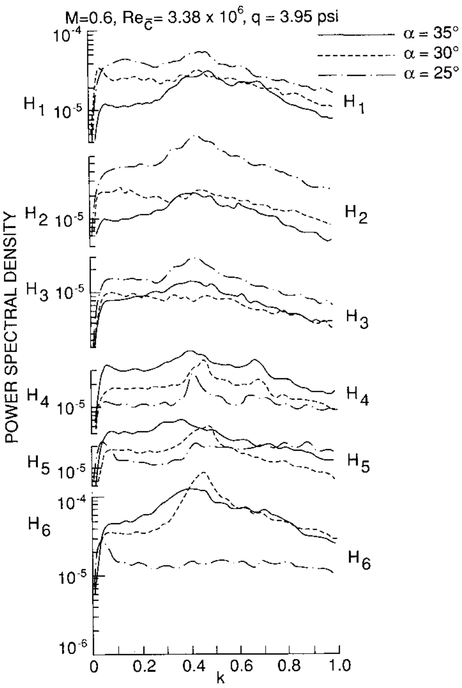

Fig. 6 Power spectral density of vortex rake horizontal array of transducers.

Along the horizontal row of unsteady transducers, Fig. 6 shows that the peak in the power spectral density plots is quite distinct at the second and third transducers, i.e., at H_2 and H_3 when $\alpha = 25$ deg. It may be seen from the total pressure contour plots shown in Fig. 3 that these two transducers are located outboard of the vertical fin and near the part of the vortex where the pressure gradient is quite large. At higher incidences, the fifth and sixth transducers (H_5 and H_6), which are located inboard of the vertical fin, show a broad peak with a value of k approximately 0.5 for $\alpha = 30$ deg, but at $\alpha = 35$ deg, the peak loses some of it distinctness.

The rms pressure fluctuations in coefficient form are shown in Fig. 7 for the horizontal row and vertical column of un-

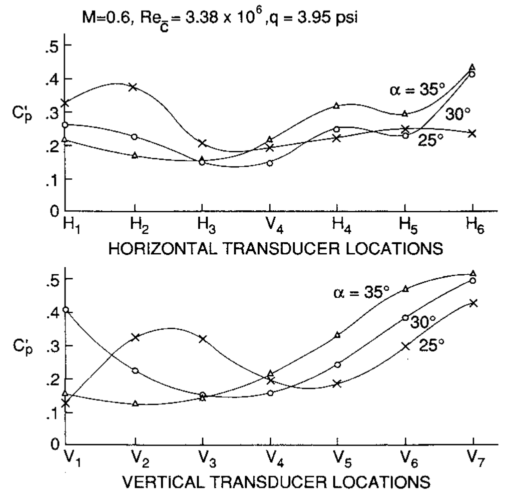

Fig. 7 C_p' distributions behind vertical fin.

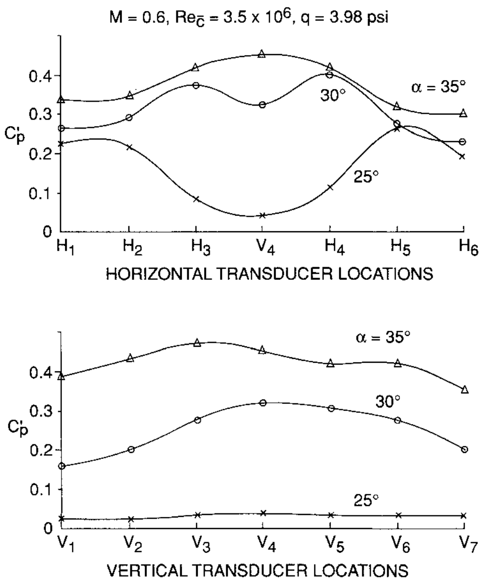

Fig. 8 C_p' distributions between vertical fins.

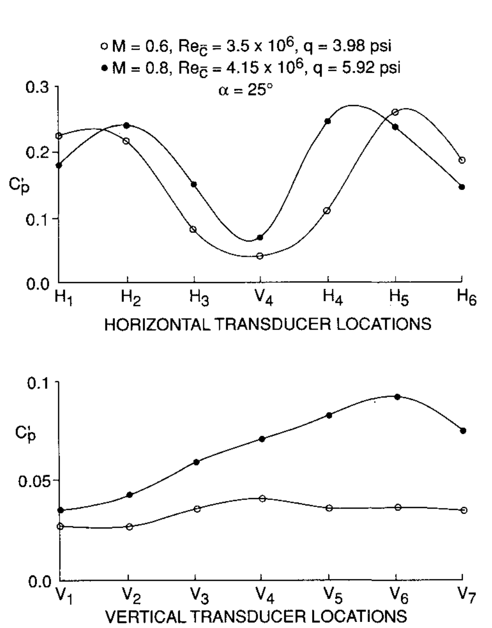

Fig. 9 C_p' distributions between vertical fins at $\alpha = 25$ deg.

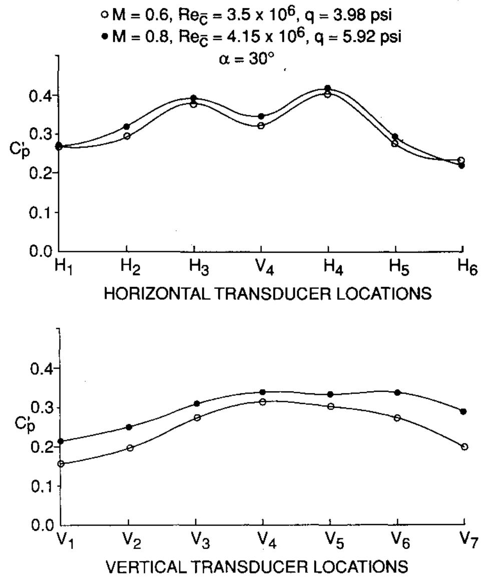

Fig. 10 C_p' distributions between vertical fins at α = 30 deg.

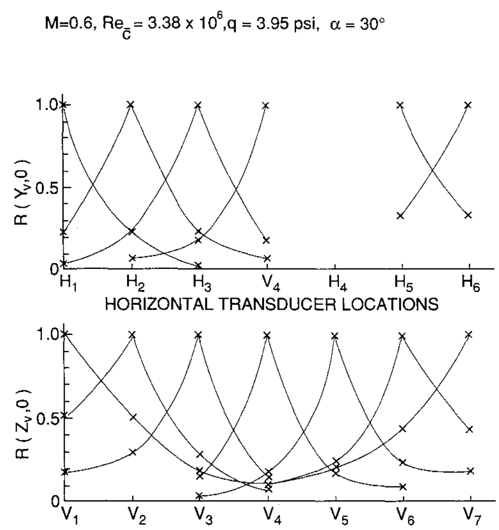

Fig. 11 Peak cross-correlation functions.

steady pressure transducers for the three values of α considered. The fin is located between the fourth and sixth transducers (V_4 and H_5) and it is seen that the fluctuations at α = 30 and 35 deg are higher at locations in the flowfield inboard of the fin surface. Along the vertical column of transducers, the pressure fluctuations are larger at the bottom near the surface of the aircraft. There are two humps on the curves at α = 25 deg. They occur in the vicinity of the vortex outboard of the vertical fin. This agrees with the observation in Ref. 1 which reported that at α = 25 deg, larger pressure fluctuations on the outboard surface of the fin were detected, while at α approximately 30 deg and greater, the inboard surface of the fin experiences larger unsteady pressures.

With the vortex rake mounted between the vertical fins, the variations in C_p' in the horizontal and vertical directions are shown in Fig. 8. At α = 25 deg, the maximum C_p' occurs close to the inboard surface and C_p' decreases towards the plane of symmetry and reaches a minimum in the middle. The maximum C_p' at α = 30 deg occurs further inwards than that at 25 deg (at transducers H_3 and H_4) and a minimum is also observed at the plane of symmetry. At α = 35 deg, a maximum is observed at the plane of symmetry and the general shape of the curve is opposite to that seen at α = 25 deg. The distributions for the three values of α are quite symmetrical. Along the vertical column of transducers C_p' for α = 25 deg is small and hardly varies from V_1 to V_7. The values of C_p' increases with α and a maximum is reached at approximately the center of the rake (at transducer location V_4).

The effects of Mach number on C_p' are shown in Figs. 9 and 10 for α = 25 and 30 deg. Results for α = 35 deg are not available. At α = 25 deg larger values of C_p' are observed for M = 0.8 than at M = 0.6. The differences between them decrease as α is increased, and at α = 30 deg the C_p' curves are much closer to each other than those at 25 deg. Generally, the values of C_p' are much higher at 30 deg than at 25 deg especially along the vertical column of transducers.

Broadband cross-correlations for various combinations of transducer pairs in the horizontal and vertical directions have been carried out. No convection in the plane of the rake was detected and this indicates that the pressure field is being convected solely in the freestream direction. In Fig. 11 the peak correlation functions vs distance are plotted and they are normalized with respect to the auto-correlation function at the reference transducer. The scale of the eddies in the pressure field is taken to be the distance measured from the reference transducer to a location in the horizontal or vertical

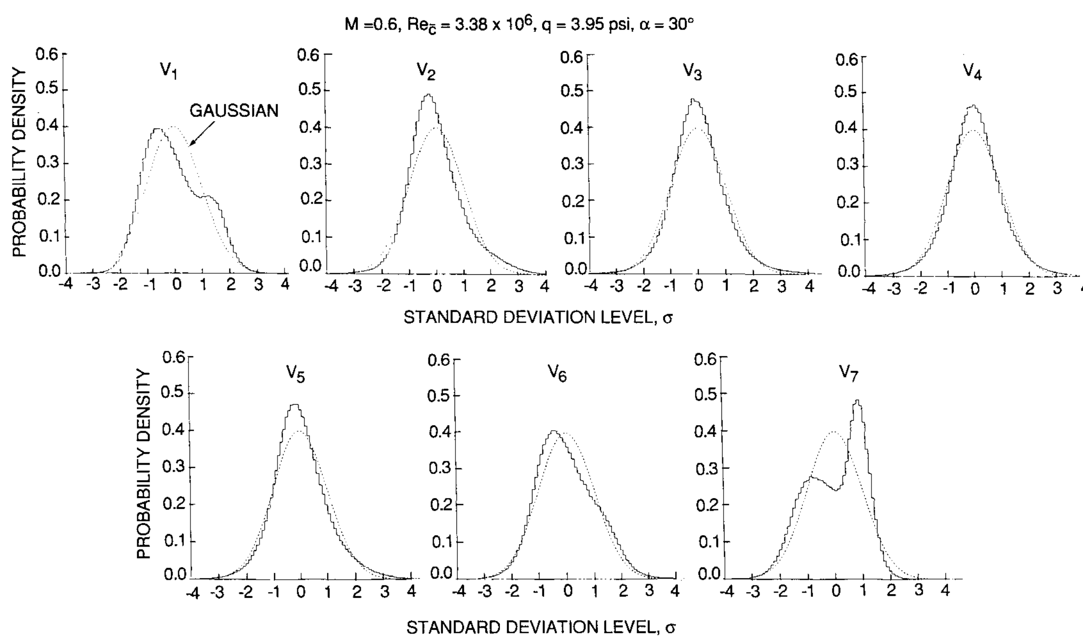

Fig. 12 Vortex rake vertical array of transducers' probability density.

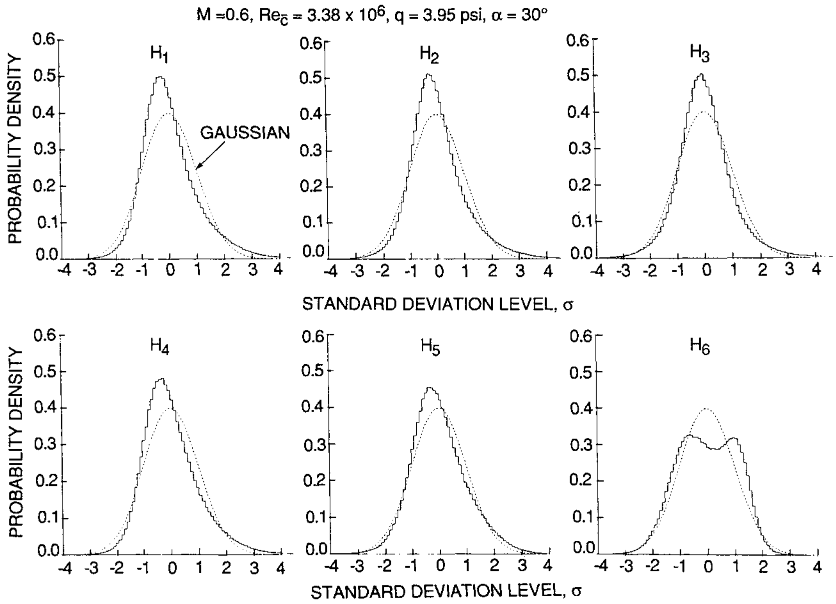

Fig. 13 Vortex rake horizontal array of transducers' probability density.

directions where the correlation function has decreased to 1/e of its value at the reference transducer. It was found that the scales at different positions in the vortical flowfield are not constant. They lie between 0.5–1.4 in., which are the extreme values. These values are only approximate since the probes are 1-in. apart and the spatial resolution is not fine enough to determine the eddy scale accurately. There is a region behind the fin between transducers V_4 and H_5 where a phase reversal in the correlation functions of 180 deg was observed. Correlation function vs time curves (not shown) demonstrate that the pressure signals behaved like band-limited noise. In experiments carried out with the vertical fin removed, it was found that the phase reversal was not observed. The presence of the vertical fin shifted the phase of the pressure signal at a location inside this region, e.g., at H_4, by 180 deg relative to that when the fin is not installed. This occurs only in the horizontal direction.

A useful statistical property of the flowfield is the probability density. In dealing with random functions, simplifications to the analysis can very often be made if the process is approximated as Gaussian. Figure 12 shows the probability densities at $M = 0.6$ and $\alpha = 30$ deg for the vertical column of transducers with the rake mounted behind the vertical fin. The uppermost transducer V_1 has the peak distribution shifted to the left. The rest of the transducers (V_2–V_6) show a fair resemblance to a Gaussian distribution except for V_7 where positive peaks at about one σ have the highest occurrence. This deviation is probably due to effects of the fuselage on the flowfield.

Figure 13 shows that along the horizontal row of transducers, in which H_1 is furthest from the plane of symmetry, the distributions are close to those for a Gaussian process for transducers H_1–H_5. The results show that the probability of finding a value of the pressure close to a level of zero is higher than a Gaussian process. At the last transducer location closest to the plane of symmetry (H_6), the distribution indicates the presence of a sinusoidal component in the pressure-time history.

IV. Conclusions

Total pressure contours and rms pressures of the vortex flowfield measured on the horizontal and vertical centerlines of the rake are presented for three angles of incidence. Higher pressure fluctuations in the flowfield are observed on the inboard side of the vertical fin at $\alpha = 30$ and 35 deg. At $\alpha = 25$ deg the vortex center is located outboard of the vertical fin and larger pressure fluctuations are observed on the outboard side. Above $\alpha = 30$ deg, pressure fluctuations measured with the rake mounted between the vertical fins, show quite similar results for $M = 0.6$ and 0.8.

Some representative results from statistical analyses of the unsteady pressures are given at $M = 0.6$ and $\alpha = 30$ deg. Spectral studies of the vortical flowfield's unsteady pressures show there are regions where a broad peak with a centered reduced frequency of approximately 0.5 is detected. Cross-correlation analyses indicate the pressure field to be convected mainly in the freestream direction. The scale of the eddies is not constant at different locations in the flowfield, but varies between 10–27% of the fin mean aerodynamic chord. With the vortex rake mounted behind the vertical fin, the probability densities of the unsteady transducers' signals show that the pressure fluctuations in most of the flowfield can be approximated by a Gaussian distribution.

Acknowledgments

The authors are indebted to the Institute for Aerospace Research for support in the high-angle-of-attack research project. The Department of National Defence provided funds for the construction of the model.

References

[1]Lee, B. H. K., and Brown, D., "Wind Tunnel Studies of F/A-18 Tail Buffet," *Journal of Aircraft*, Vol. 29, No. 1, 1992, pp. 146–152.

[2]Lee, B. H. K., Brown, D., Zgela, M., and Poirel, D., "Wind Tunnel Investigation and Flight Tests of Tail Buffet on the CF-18 Aircraft," *Aircraft Dynamic Loads Due to Flow Separation*, AGARD-CP-483, Sorrento, Italy, April 1990.

[3]Brown, D., Lee, B. H. K., and Tang, F. C., "Some Characteristics and Effects of the F/A-18 LEX Vortices," *Vortex Flow Aerodynamics*, AGARD-CP-494, Scheveningen, The Netherlands, Oct. 1990.

[4]Lee, B. H. K., and Dunlavy, S., "Statistical Prediction of Maximum Buffet Loads on the F/A-18 Vertical Fin," *Journal of Aircraft*, Vol. 29, No. 4, 1992, pp. 734–736.

[5]Lee, B. H. K., "A Method for Predicting Wing Response to Buffet Loads," *Journal of Aircraft*, Vol. 21, No. 1, 1984, pp. 85–87.

[6]Wentz, W. H., Jr., "Vortex-Fin Interaction on a Fighter Aircraft," AIAA 5th Applied Aerodynamics Conf., AIAA Paper 87-2474, Monterey, CA, Aug. 1987.

[7]Erickson, G. E., Hall, R. M., Banks, D. W., Del Frate, J. H., Schreiner, J. A., Hanely, R. J., and Pulley, C. T., "Experimental Investigation of the F/A-18 Vortex Flows at Subsonic Through Transonic Speeds, Invited Paper," AIAA 7th Applied Aerodynamics Conf., AIAA Paper 89-2222, Seattle, WA, July–Aug. 1989.

[8]Sellers, W. L., III, Meyers, J. F., and Hepner, T. E., "LDV Surveys over a Fighter Model at Moderate to High Angles of Attack," Aerospace Technology Conf. and Exposition, Society of Automotive Engineers TP 881448, Anaheim, CA, Oct. 1988.